

Supporting Information

Azacalixpyrins as an Innovative Alternative for the Free-Radical Photopolymerization under Visible and NIR Irradiation without the Need of Co-Initiators

Louise Breloy,^a Rana Mhanna,^b Jean-Pierre Malval,^b Vlasta Brezova,^c Denis Jacquemin,^{*d} Simon Pascal,^e Olivier Siri,^{*e} Davy-Louis Versace^{*a}

^a Institut de Chimie et des Matériaux Paris-Est (UMR-CNRS 7182-UPEC), 2-8 rue Henri Dunant, 94320 Thiais

^b Institut de Science des Matériaux de Mulhouse (IS2M) (UMR-CNRS 7361), 15, rue Jean Starcky, 68057 Mulhouse

^c Slovak University of Technology in Bratislava, Faculty of Chemical and Food Technology, Institute of Physical Chemistry and Chemical Physics, Department of Physical Chemistry, Radlinského 9, SK-812 37 Bratislava, Slovak Republic

^d Université de Nantes, CEISAM UMR 6230, CNRS, F-44000 Nantes, France

^e Aix Marseille Univ, CNRS UMR 7325, Centre Interdisciplinaire de Nanoscience de Marseille (CINaM), Campus de Luminy, case 913, 13288 Marseille cedex 09, France

Experimental section.....	S3
Figures.....	S6
Tables.....	S16
References.....	S17

Experimental section

Materials. **ACP** was synthesized according to a reported procedure (^1H NMR spectrum in Figure S9).¹ Soybean oil acrylate (SOA, Figure S10), 5,5-dimethyl-1-pyrroline *N*-oxide (DMPO) and α -(4-pyridyl*N*-oxide)-*N*-*tert*butylnitron (POBN) were provided from Sigma Aldrich.

EPR experiments. The X-band cw-EPR spectra (modulation frequency of 100 kHz) were monitored with an EMX*plus* spectrometer (Bruker) equipped with the High Sensitivity Probe-head (Bruker) in the small quartz flat cell (WilmaD-LabGlass, WG 808-Q). The solutions prepared in dimethylsulfoxide (DMSO, anhydrous, Sigma-Aldrich) or methanol (anhydrous, Sigma-Aldrich) and carefully saturated with argon were irradiated at 295 K directly in the EPR resonator using LED@450 nm (KL1600LED, Schott, blue filter) or LED@VIS (KL1600LED, Schott, full spectrum) source. The EPR spectra were recorded *in situ* during/after a defined exposure as described previously.² The 5,5-dimethyl-1-pyrroline *N*-oxide (DMPO, Sigma-Aldrich, distilled and stored at $-20\text{ }^\circ\text{C}$ before the application) or α -(4-pyridyl *N*-oxide)-*N*-*tert*-butylnitron (POBN; Sigma-Aldrich) were applied as the spin trapping agents. The *g*-factors were determined with an uncertainty of ± 0.0001 exploiting a nuclear magnetic resonance teslameter (ER 036TM, Bruker) and integrated frequency counter. The experimental EPR spectra were analyzed by the WinEPR software (Bruker) and the calculations of spin-Hamiltonian parameters and relative concentrations of individual DMPO-adducts were performed with the EasySpin toolbox working on MatLab[®] platform.³

UV-Vis-NIR spectroscopy. UV-Visible spectrum of **ACP** in methanol was reported from a previous work.⁴

Photopolymerization. Photopolymerizable formulation was composed of 0.5 wt% of **ACP** in soybean oil epoxidized acrylate. The kinetics of polymerization were recorded by Real Time Fourier Transform InfraRed (RT-FTIR) spectroscopy on a JASCO FTIR 4700 Instrument. Formulation was deposited on a BaF₂ pellet (from Korth Kristalle GMBH), with a constant thickness of 25 μm . Laminate conditions were obtained by isolation of the photosensitive layer with a propylene film, without any previous degassing. Monomer conversion was followed by the integration of the acrylate double bond signal at 1635 cm^{-1} . Irradiation sources were LED@455 nm (55 $\text{mW}\cdot\text{cm}^{-2}$, 10 $\text{mW}\cdot\text{cm}^{-2}$), LED@470 nm (35 $\text{mW}\cdot\text{cm}^{-2}$, 10 $\text{mW}\cdot\text{cm}^{-2}$), LED@505 nm (20 $\text{mW}\cdot\text{cm}^{-2}$, 10 $\text{mW}\cdot\text{cm}^{-2}$), LED@590 nm (50 $\text{mW}\cdot\text{cm}^{-2}$, 10 $\text{mW}\cdot\text{cm}^{-2}$), LED@625 nm (45 $\text{mW}\cdot\text{cm}^{-2}$, 10 $\text{mW}\cdot\text{cm}^{-2}$) and LED@660 nm (10 $\text{mW}\cdot\text{cm}^{-2}$) provided by Thorlabs Instruments.

Final conversions and initial rates of polymerization were calculated according to the following equations:

$$\text{FC (\%)} = 100 \times \frac{A(t=0) - A(t)}{A(0)} \quad (\text{ES1}) \quad \text{and} \quad R_p = \frac{[M]_0}{t} \times \frac{A(t=0) - A(t)}{A(0)} \quad (\text{ES2})$$

With FC final conversion (%), $A(t)$ absorbance at time t of irradiation, R_p initial polymerization rate ($\text{mol.L}^{-1}.\text{s}^{-1}$), $[M]_0$ concentration in acrylate functions in the monomer (mol.L^{-1}), t time (s).

Calculation of absorbed photon flux was calculated using the following equations⁵:

$$\Phi = \frac{H}{qE} \quad (\text{ES3})$$

With Φ = photon flux = number of photons emitted by the lamp/ s.m^2 (photon/s.m^2), H = power density (W.m^{-2}), E energy of the photons (eV), and q electronic charge.

$$A = -\log(T) = \epsilon l C \quad (\text{ES4})$$

With A absorbance of the solution at fixed wavelength, T transmittance, ϵ molar extinction coefficient ($\text{L.mol}^{-1}.\text{s}^{-1}$), and C the concentration of **ACP** (mol.L^{-1}).

$$\Phi_{\text{abs}} = (1-T) \times \Phi \quad (\text{ES5})$$

With Φ_{abs} the absorbed photon flux (photon/s.m^2) and $(1-T)$ proportion of the photons absorbed.

Microfabrication. The NIR lithographic microfabrication was carried out using a 3D-stereolithography (SLA) set-up purchased from Microlight3D Company. The set-up was optically adapted for NIR excitation. We used a Zeiss Axio Observer D1 inverted microscope. The NIR excitation was performed at 800 nm using respectively a mode-locked Ti:Sapphire oscillator (Coherent, Chameleon Ultra II: pulse duration: ~ 140 fs; repetition rate: 80 MHz). The incident beam was focused through a 0.65 numerical aperture objective (40 X) which leads to a radial spot size 600 nm at $\lambda_{\text{exc}} = 800$ nm ($1/e^2$ Gaussian). The excitation input power was maintained at 4.5 mW with an exposure time of 4 ms. A drop of the resin is deposited on a cover slip which is mounted on a 3D piezoelectric stage allowing the translation relative to the laser focal point. The intensity of the entering laser is controlled with the use of an acousto optic modulator. The displacement of the sample and all photonic parameters (*i.e.* excitation power and irradiation times) are computer-controlled. The microstructure is finally obtained by washing away the unexposed monomer resin using ethanol. The NIR-polymerized μ -structures was characterised using a FEI Quanta 400 scanning electron microscope. The sputter coating of the sample was performed with gold prior SEM measurements.

DFT calculations. The DFT calculations have been performed with Gaussian 16⁶, using the PBE0⁷ functional and the 6-31G(d) atomic basis set. The geometry optimizations were performed using a *tight* convergence criterion, and the *ultrafine* integration grid was selected. The nature of the obtained structures was confirmed by analytical calculations of the vibrational frequencies. The unrestricted formalism was used for the open-shell species. The vertical absorption spectrum was modelled through TD-DFT, using the same functional but a larger basis set, namely 6-31+G(d,p). The excited states are represented as electronic density difference (EDD) plots, in which the difference of the

excited state and ground state densities, as obtained with TD-DFT and DFT, respectively is given. A contour threshold of 4×10^{-4} au is used to plot these EDDs.

Figures

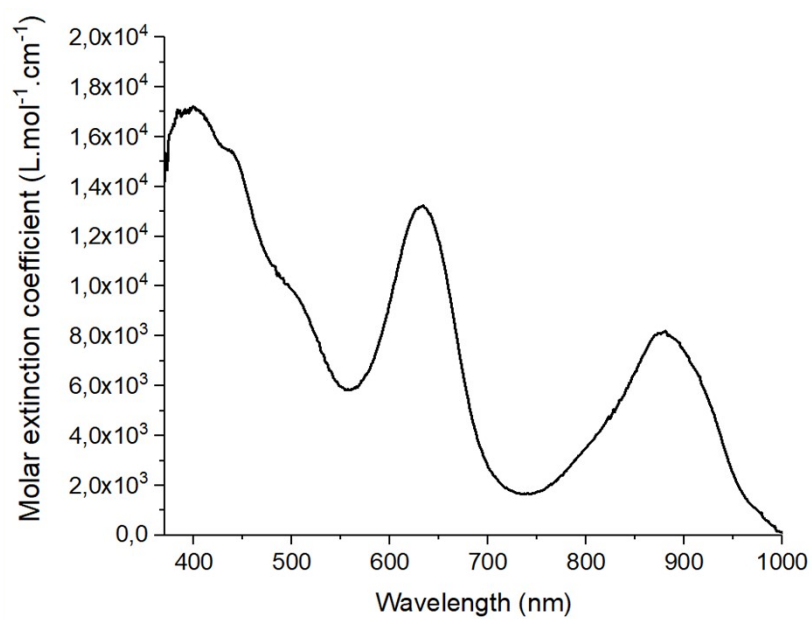


Figure S1. Absorption spectrum of **ACP** in SOA monomer (Blank: pure SOA monomer).

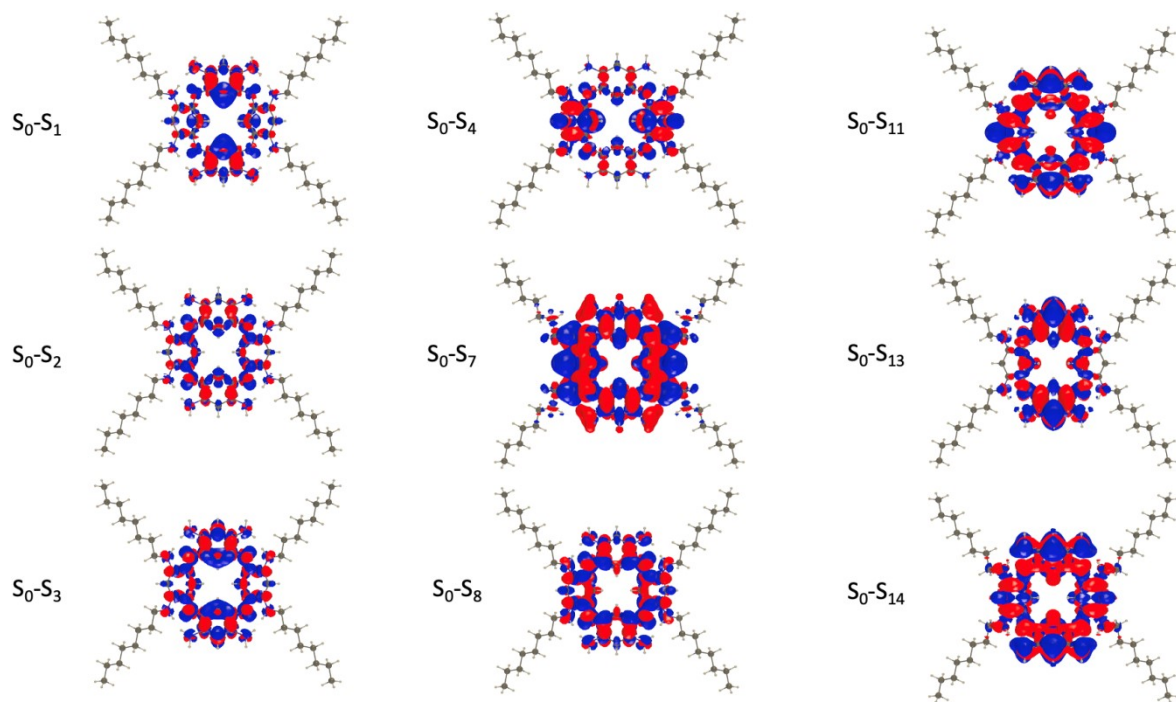


Figure S2. EDD plots for the key dipole-allowed transitions of **ACP**. The blue and red lobes represent decrease and increase of electron density upon photo-absorption, respectively.

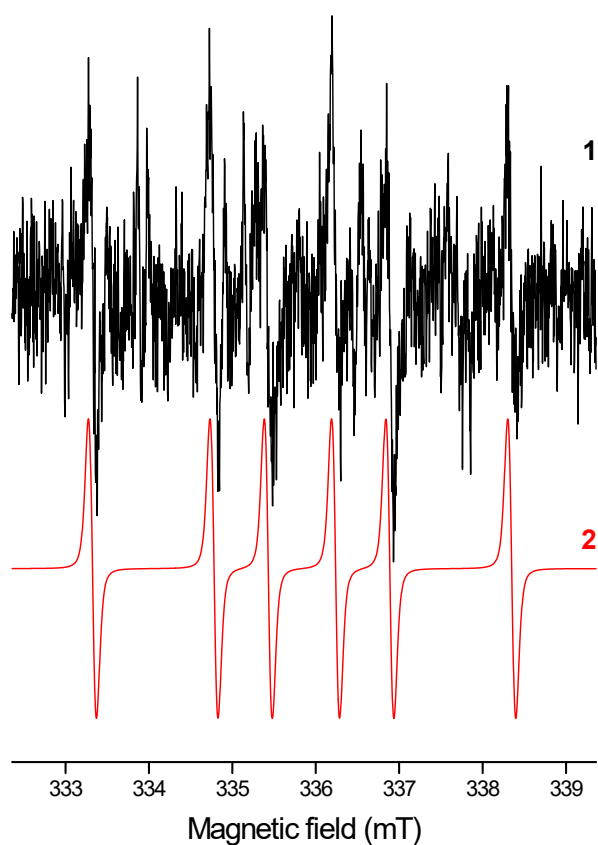


Figure S3. Normalized experimental (1) and simulated (2) EPR spectra obtained upon 1800 s *in situ* LED@VIS nm (450 nm) exposure of deoxygenated DMSO solution of **ACP** in the presence of DMPO spin trap. EPR spectrometer settings: microwave frequency, ~ 9.43 GHz; microwave power, 10.70 mW; center field, ~335.9 mT; sweep width, 7 mT; gain, 1.00×10^5 ; modulation amplitude, 0.05 mT; sweep time, 45 s; time constant, 10.24 ms; number of scans, 10.

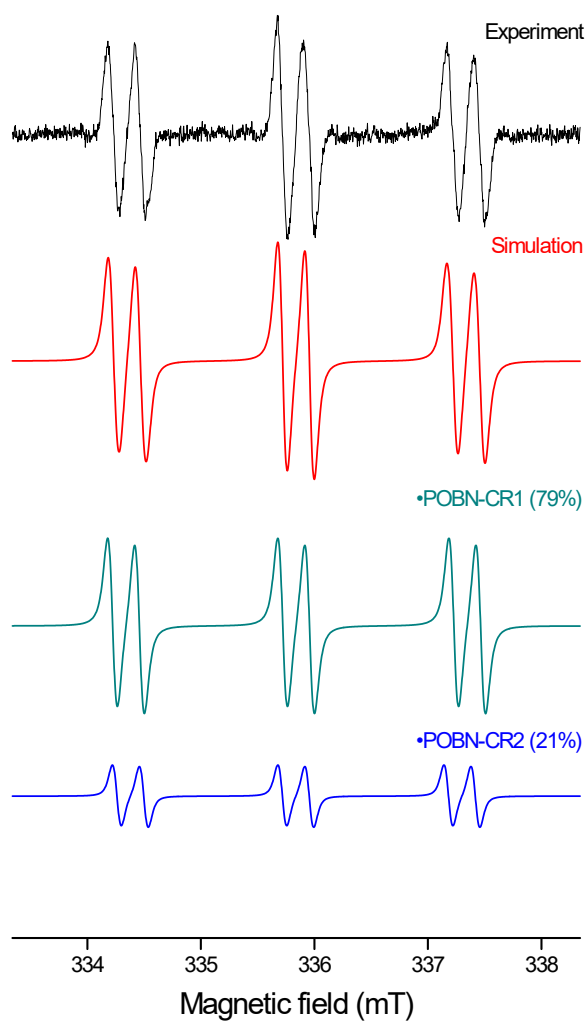


Figure S4. The experimental and simulation EPR spectra obtained after 1800 s *in situ* LED@VIS nm (450 nm) exposure of deoxygenated DMSO solution of **ACP** in the presence of POBN spin trap (black line) along with the composite simulation (red line) and its decomposition to the individual contributions (colored lines). •POBN-CR1: $a_N = 1.506$ mT, $a_H^\beta = 0.238$ mT; $g = 2.0061$; $\Delta B_{pp,G} = 0.055$ mT, $\Delta B_{pp,L} = 0.051$ mT; relative concentration 79%. •POBN-CR2: and $a_N = 1.464$ mT, $a_H^\beta = 0.238$ mT; $g = 2.0061$; $\Delta B_{pp,G} = 0.055$ mT, $\Delta B_{pp,L} = 0.040$ mT; 21%.

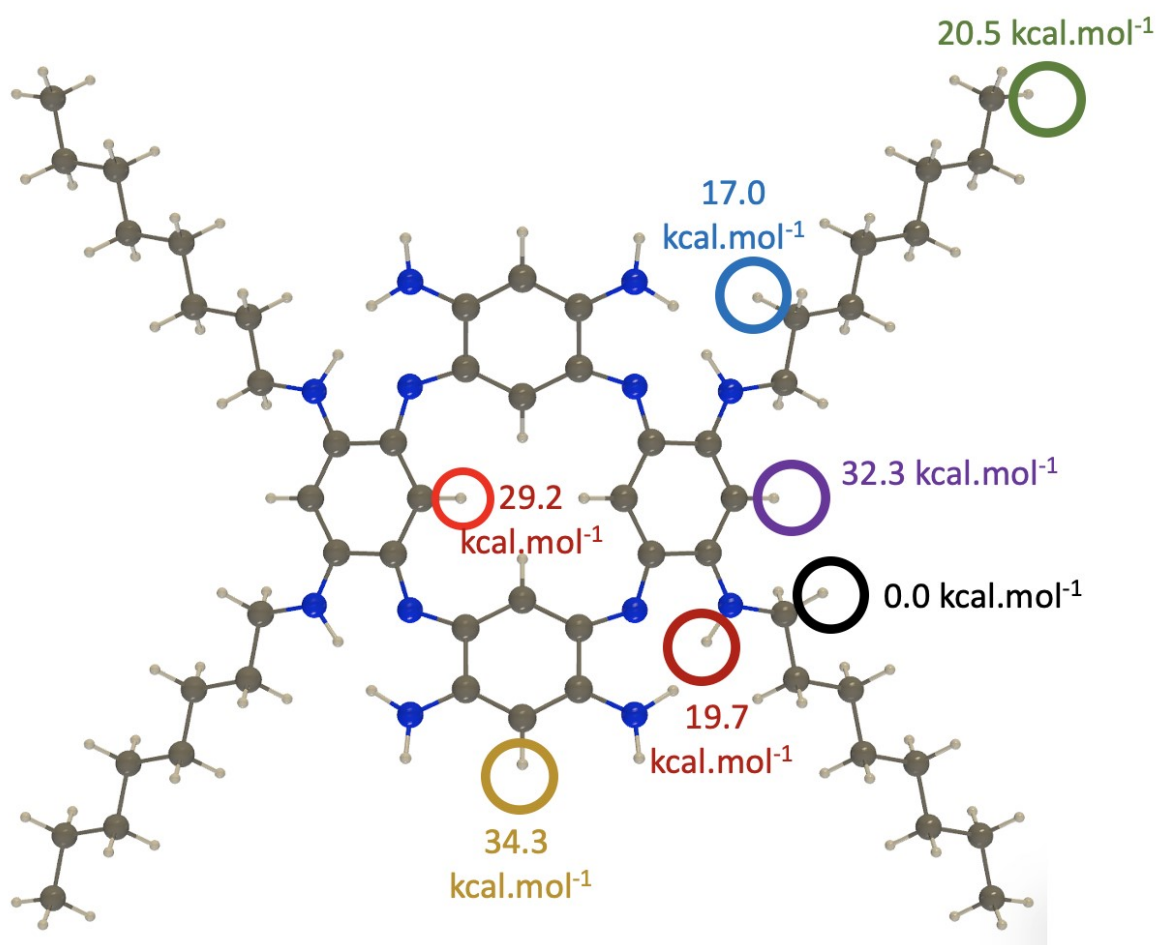


Figure S5. Relative free energies, G , of the formed radicals, as a function of the extracted H atom from **ACP**. The most stable radical is taken as reference, and all structures are fully optimized, starting with the parent (neutral) structure.

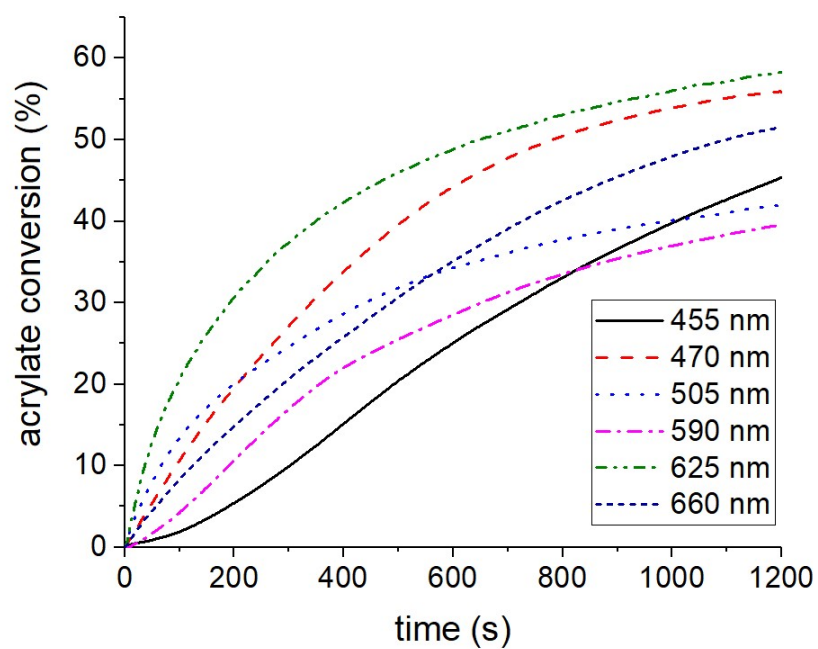


Figure S6. Kinetic profiles for the acrylate polymerization of SOA with **ACP** (0.5 wt%) photoinitiating system upon LEDs@455, 470, 505, 590, 625 and 660 nm irradiation. Light intensity = 55, 35, 20, 50, 45 and 10 $\text{mW}\cdot\text{cm}^{-2}$, respectively.

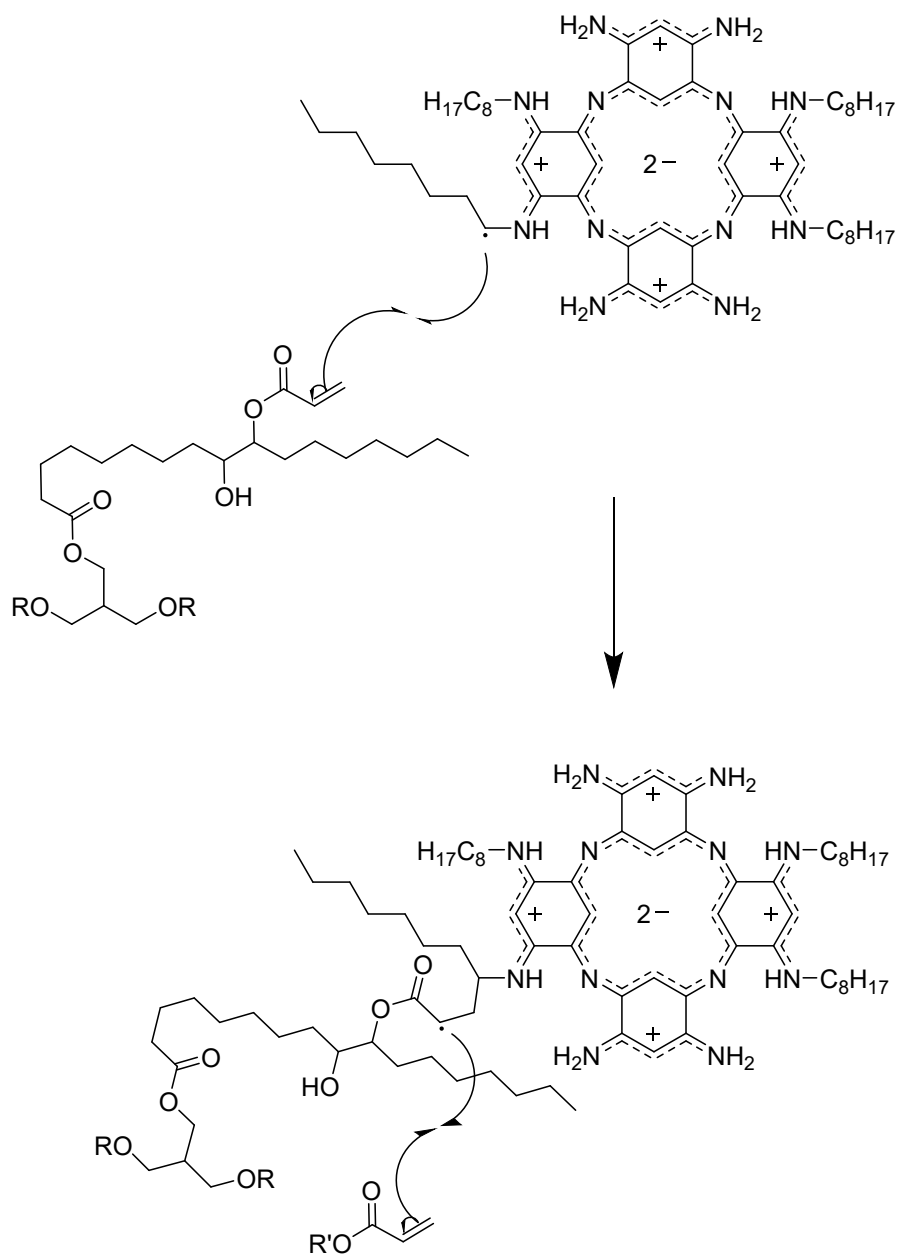


Figure S7. Initiation mechanism of SOA polymerization by ACP radical. In the theoretical calculation the substrate is modelled as a simple methyl acrylate monomer.

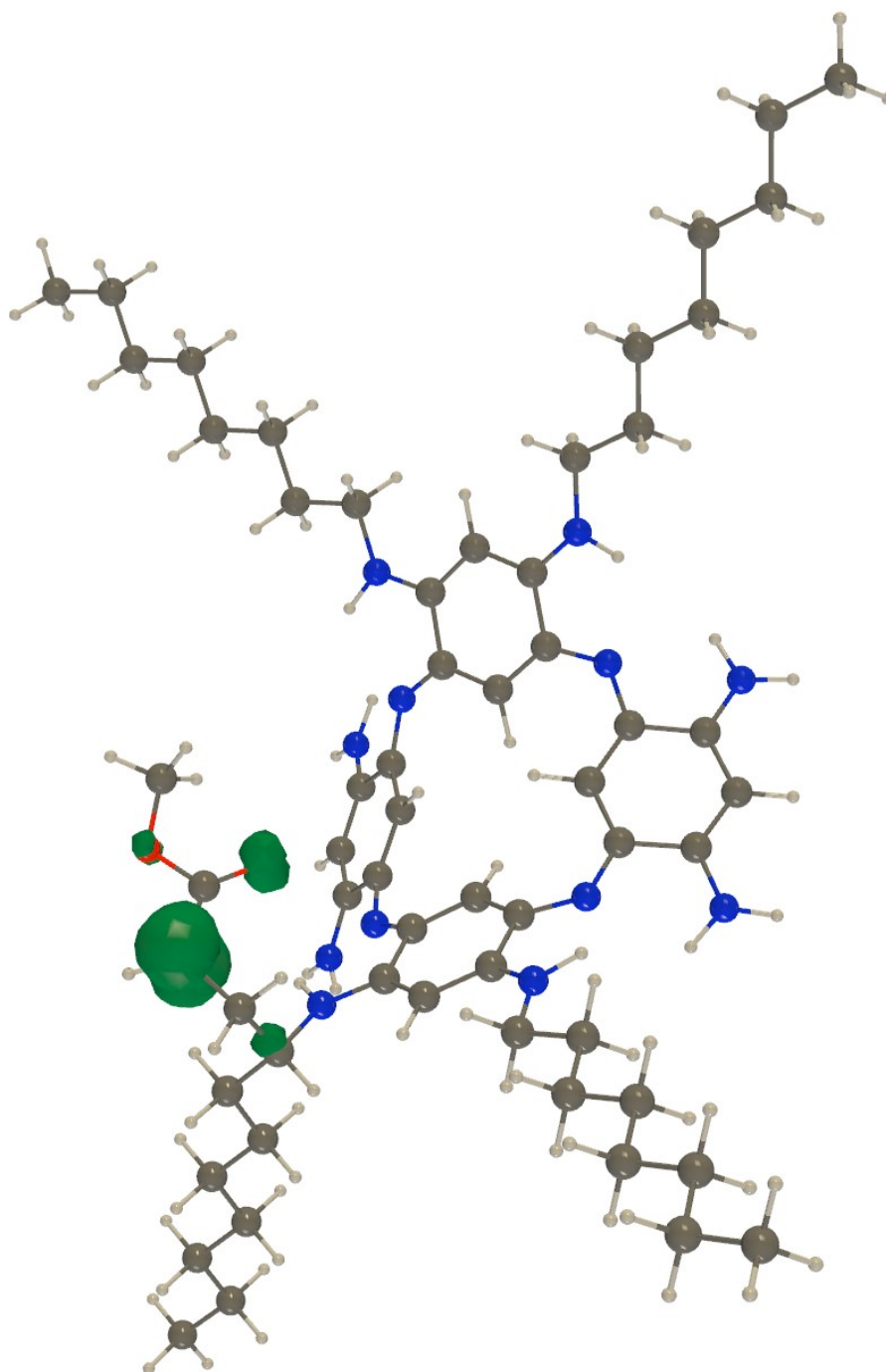


Figure S8. Spin density difference plot of the product between **ACP** and methyl acrylate, showing the localization of the spin density on the latter, allowing for the polymerization to continue. Contour threshold: 0.008 au.

SP512-precAcetone-CD3OD
single_pulse

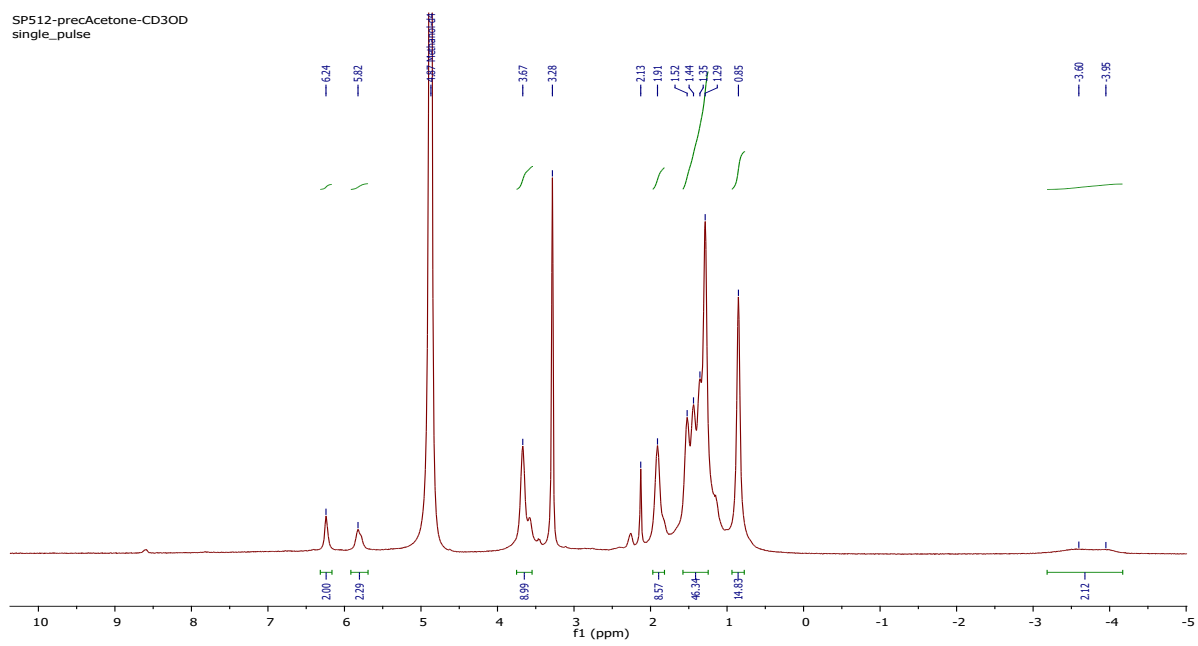


Figure S9. ^1H NMR spectrum of ACP

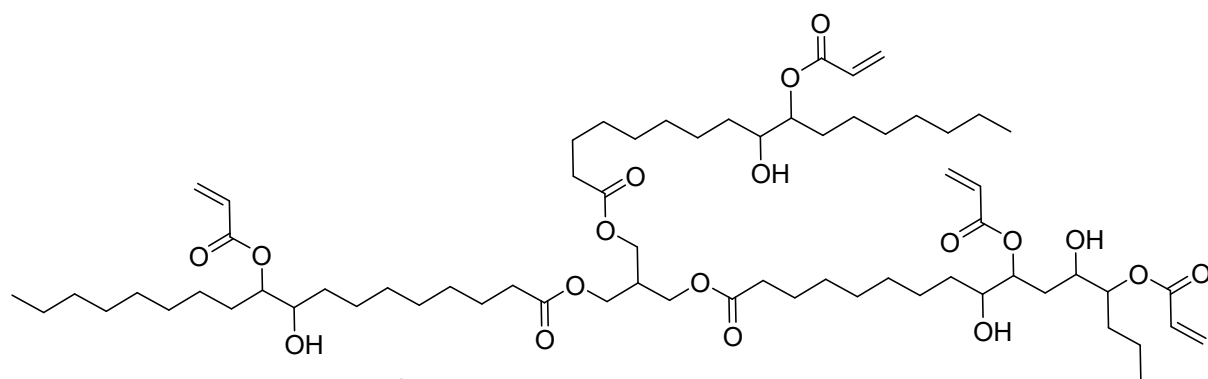


Figure S10. Chemical structure of SOA.

Tables

Table S1. Molar extinction coefficients of **ACP** at the emission wavelength of several LEDs in methanol

LED λ_{max} (nm)	455	470	505	590	625	660	800
ϵ (L.mol ⁻¹ .cm ⁻¹)	19700	17300	14600	10200	18400	21900	6000

Table S2. TD-PBE0/6-31+G(d,p) vertical excitation wavelength of **ACP**. We provide also the oscillator strength (f). Only the states with a non-negligible f are listed

Transition	λ (NM)	F
S ₀ -S ₁	795	0.025
S ₀ -S ₂	785	0.097
S ₀ -S ₃	590	0.453
S ₀ -S ₄	578	0.174
S ₀ -S ₇	497	0.023
S ₀ -S ₈	482	0.086
S ₀ -S ₁₁	433	0.263
S ₀ -S ₁₃	400	0.384
S ₀ -S ₁₄	383	0.152

Table S3. Final acrylate conversions of SOA (determined by FTIR), initial rate of polymerizations, and absorbed photon flux in the presence of **ACP** (0.5 wt%) at 10 mW.cm⁻² and under different LEDs intensities in laminate after 1200 s of irradiation.

LED λ_{MAX} (nm)	455	470	505	590	625	660
$\Phi_{\text{abs}} \times 10^{-19}$ (FOR 10 mw.cm ⁻²)	18.5	18.2	18.1	18.4	25.0	25.0
Final Conversions (%)	33 (46)	20 (56)	22 (42)	20 (28)	47 (58)	51 (51)
$100 \times R_p/[M]_0$ (mol. L ⁻¹ .s ⁻¹)	1.6 (4.5)	0.3 (29.8)	2.6 (13.1)	2.8 (5.4)	13.0 (27.3)	8.0 (8.0)

() = conversions under LEDs@455, 470, 505, 590, 625 and 660 nm irradiation at maximum light intensity of 55, 35, 20, 50, 45 and 10 mW.cm⁻² respectively.

References

1. Chen, Z.; Haddoub, R.; Mahe, J.; Marchand, G.; Jacquemin, D.; Andeme Edzang, J.; Canard, G.; Ferry, D.; Grauby, O.; Ranguis, A.; Siri, O., N-Substituted Azacalixphyrins: Synthesis, Properties, and Self-Assembly. *Chemistry* 2016, **22**, 17820.
2. Marcille, H.; Malval, J.-P.; Pisset, M.; Bogliotti, N.; Blacha-Grzechnik, A.; Brezová, V.; Yagci, Y.; Versace, D.-L., Diphenyl functional porphyrins and their metal complexes as visible-light photoinitiators for free-radical, cationic and thiol-ene polymerizations. *Polym. Chem.* 2020, **11**, 4237.
3. Stoll, S.; Schweiger, A., EasySpin, a comprehensive software package for spectral simulation and analysis in EPR. *J. Magn. Reson.* 2006, **178**, 42.
4. Lavaud, L.; Pascal, S.; Metwally, K.; Gasteau, D.; Da Silva, A.; Chen, Z.; Elhabiri, M.; Canard, G.; Jacquemin, D.; Siri, O., Azacalixphyrins as NIR photoacoustic contrast agents. *Chem. Comm. (Camb)* 2018, **54**, 12365.
5. Stafford, A.; Ahn, D.; Raulerson, E. K.; Chung, K. Y.; Sun, K.; Cadena, D. M.; Forrister, E. M.; Yost, S. R.; Roberts, S. T.; Page, Z. A., Catalyst Halogenation Enables Rapid and Efficient Polymerizations with Visible to Far-Red Light. *J. Am. Chem. Soc.* 2020, **142**, 14733.
6. Frisch, M. J.; Trucks, G. W.; Schlegel, H. B.; Scuseria, G. E.; Robb, M. A.; Cheeseman, J. R.; Scalmani, G.; Barone, V.; Petersson, G. A.; Nakatsuji, H.; Li, X.; Caricato, M.; Marenich, A. V.; Bloino, J.; Janesko, B. G.; Gomperts, R.; Mennucci, B.; Hratchian, H. P.; Ortiz, J. V.; Izmaylov, A. F.; Sonnenberg, J. L.; Williams-Young, D.; Ding, F.; Lipparini, F.; Egidi, F.; Goings, J.; Peng, B.; Petrone, A.; Henderson, T.; Ranasinghe, D.; Zakrzewski, V. G.; Gao, J.; Rega, N.; Zheng, G.; Liang, W.; Hada, M.; Ehara, M.; Toyota, K.; Fukuda, R.; Hasegawa, J.; Ishida, M.; Nakajima, T.; Honda, Y.; Kitao, O.; Nakai, H.; Vreven, T.; Throssell, K.; Montgomery, J. A.; Peralta, J., J. E.; Ogliaro, F.; Bearpark, M. J.; Heyd, J. J.; Brothers, E. N.; Kudin, K. N.; Staroverov, V. N.; Keith, T. A.; Kobayashi, R.; Normand, J.; Raghavachari, K.; Rendell, A. P.; Burant, J. C.; Iyengar, S. S.; Tomasi, J.; Cossi, M.; Millam, J. M.; Klene, M.; Adamo, C.; Cammi, R.; Ochterski, J. W.; Martin, R. L.; Morokuma, K.; Farkas, O.; Foresman, J. B.; Fox, D. J., Gaussian 16.A03. Wallingford, USA 2016.
7. Adamo, C.; Barone, V., Toward reliable density functional methods without adjustable parameters: The PBE0 model. *J. Chem. Phys.* 1999, **110**, 6158.